UC San Diego
UC San Diego Previously Published Works

## Title

# Quantitative Imaging Biomarkers of Damage to Critical Memory Regions Are Associated With Post–Radiation Therapy Memory Performance in Brain Tumor Patients

## Permalink

https://escholarship.org/uc/item/3rk9f19n

## Journal

International Journal of Radiation Oncology • Biology • Physics, 105(4)

## ISSN

0360-3016

## Authors

Tringale, Kathryn R
Nguyen, Tanya T
Karunamuni, Roshan
et al.

## Publication Date

2019-11-01

## DOI

10.1016/j.ijrobp.2019.08.003

Peer reviewed

eScholarship.org Powered by the California Digital Library
University of California

Author Manuscript
Author Manuscript
Author Manuscript
Author Manuscript

HHS Public Access

Author manuscript

*Int J Radiat Oncol Biol Phys*. Author manuscript; available in PMC 2020 November 15.

Published in final edited form as:

*Int J Radiat Oncol Biol Phys*. 2019 November 15; 105(4): 773–783. doi:10.1016/j.ijrobp.2019.08.003.

# Quantitative imaging biomarkers of damage to critical memory regions associated with post-radiotherapy memory performance in brain tumor patients

**Kathryn R. Tringale, MD, MAS**[1], **Tanya T. Nguyen, PhD**[3], **Roshan Karunamuni, PhD**[1,2], **Tyler Seibert, MD, PhD**[1,2], **Minh-Phuong Huynh-Le, MD**[1], **Michael Connor, MD**[1], **Vitali Moiseenko, PhD**[1], **Mary Kay Gorman, RN**[1], **Anisa Marshall, BS**[2], **Michelle Devereux Tibbs, BS**[1], **Nikdokht Farid, MD**[4], **Daniel Simpson, MD**[1], **Parag Sanghvi, MD**[1], **Carrie R. McDonald, PhD**[1,2,3,*], **Jona A. Hattangadi-Gluth, MD**[1,2,*]

[1]Department of Radiation Medicine and Applied Sciences, University of California, San Diego, La Jolla, CA, USA 92093

[2]Center for Multimodal Imaging and Genetics, University of California, San Diego, La Jolla, CA, USA 92093

[3]Department of Psychiatry, University of California, San Diego, La Jolla, CA, USA 92093

[4]Department of Radiology, University of California, San Diego, La Jolla, CA, USA 92093

## Abstract

**Purpose:** We used quantitative MRI to prospectively analyze the association between microstructural damage to memory-associated structures within the medial temporal lobe and longitudinal memory performance after brain radiotherapy (RT).

**Methods and Materials:** Primary brain tumor patients receiving fractionated brain RT were enrolled on a prospective trial (n=27). Patients underwent high resolution volumetric brain MRI, diffusion-weighted imaging, and neurocognitive testing prior to and 3, 6, and 12 months post-RT.

---

[*]These authors contributed equally as senior authors

**Corresponding Author:** Jona A. Hattangadi-Gluth, University of California, San Diego, Moores Cancer Center, Department of Radiation Medicine and Applied Sciences, 3960 Health Sciences Drive #0865, La Jolla, CA 92093-0843, Phone: (858) 534- 12223, Fax: (858) 822-6081, jhattangadi@ucsd.edu.

Author Contributions:
Concept and design: KRT, JAH-G, CRM, RK, TN
Acquisition, analysis, or interpretation of data: All authors.
Drafting of the manuscript: All authors.
Statistical analysis: KRT, TN
Obtained funding: JAH-G, CRM
Administrative, technical, or material support: JAH-G, CRM

**Publisher's Disclaimer:** This is a PDF file of an unedited manuscript that has been accepted for publication. As a service to our customers we are providing this early version of the manuscript. The manuscript will undergo copyediting, typesetting, and review of the resulting proof before it is published in its final citable form. Please note that during the production process errors may be discovered which could affect the content, and all legal disclaimers that apply to the journal pertain.

**Meeting Presentations:** A version of this analysis was previously presented orally at the 2017 annual American Society of Radiation Oncology meeting in San Diego, CA.

**Potential conflicts of interest:** JAH-G has research funding from Varian Medical Systems (Palo Alto, CA), unrelated to the current study. CRM has research funding from GE Healthcare, unrelated to the current study.

Author Manuscript Author Manuscript Author Manuscript Author Manuscript

Medial temporal lobe regions (hippocampus; entorhinal, parahippocampal, and temporal pole white matter [WM]) were auto-segmented, quantifying volume and diffusion biomarkers of WM integrity (mean diffusivity [MD]; fractional anisotropy [FA]). Reliable change indices (RCI) measured changes in verbal (Hopkins Verbal Learning Test-Revised [HVLT-R]) and visuospatial (Brief Visuospatial Memory Test-Revised [BVMT-R]) memory. Linear mixed-effects models assessed longitudinal associations between imaging parameters and memory.

**Results:** Visuospatial memory significantly declined at 6 months post-RT (mean RCI - 1.3, $P$=.012). Concurrent chemotherapy and seizures trended toward a significant association with greater decline in visuospatial memory ($P$=.053, $P$=.054, respectively).

Higher mean dose to the left temporal pole WM was significantly associated with decreased FA ($r$=−.667, $P$=.002). Over all time points, smaller right hippocampal volume ($P$=.021), lower right entorhinal FA ($P$=.023), greater right entorhinal MD ($P$=.047), and greater temporal pole MD (BVMT-R Total Recall, $P$=.003; BVMT-R Delayed Recall, $P$=.042) were associated with worse visuospatial memory. The interaction between right entorhinal MD (BVMT-R Total Recall, $P$=.021; BVMT-R Delayed Recall, $P$=.004), and temporal pole FA (BVMT-R Delayed Recall, $P$=.024) significantly predicted visuospatial memory performance.

**Conclusions:** Brain tumor patients exhibited visuospatial memory decline post-RT. Microstructural damage to critical memory regions, including the hippocampus and medial temporal lobe WM, were associated with post-RT memory decline. The integrity of medial temporal lobe structures is critical to memory performance post-RT, representing possible avoidance targets for memory preservation.

**Keywords**

radiation therapy; brain tumor; neuroimaging; memory

## INTRODUCTION

Radiation therapy (RT) is a mainstay in the treatment of benign and malignant primary brain tumors. However, RT can result in post-treatment neurocognitive decline[1], most frequently reported in verbal and visuospatial memory (i.e., difficulty encoding, retaining, and retrieving visual information). Neurocognitive decline has been shown to be an independent predictor of survival for patients with brain tumors, and the late delayed (6 months and greater) effects of RT are typically irreversible and progressive[1]. Thus, neurocognitive outcomes have become a critical endpoint in brain RT clinical trials[2].

Radiation-induced injury to the brain is mediated by destruction of actively dividing progenitor cells (e.g. hippocampus), damage to white matter (WM) tracts, vascular injury, and neuroinflammation[1]. Axonal degradation and demyelination of WM has been noted on histopathologic studies after radiation exposure[3,4], and diffusion tensor imaging (DTI) biomarkers are associated with these changes. Indeed, previous DTI studies have shown regional dose-dependent WM damage[5–8] after RT: specifically, a decrease in Fractional Anisotropy (FA) and increase in Mean Diffusivity (MD) indicating loss of white matter integrity. Other studies have demonstrated associations between WM damage to certain structures (i.e., parahippocampal cingulum) and neurocognitive decline[9–11]. In addition to

Author Manuscript Author Manuscript Author Manuscript Author Manuscript

WM, gray matter structures, such as the hippocampus, exhibit dose-dependent atrophy[12] after RT and likely play a role in radiation-induced neurocognitive decline[13].

In this prospective study of primary brain tumor patients receiving fractionated brain RT, we analyzed discrete gray and WM regions involved in memory using high-resolution structural and diffusion-weighted imaging. Specifically, we investigated the association between structural and microstructural damage to medial temporal lobe regions and post-RT decline in both verbal and visuospatial learning and memory. This study is the first among those investigating adult patients with brain tumors to include visuospatial memory as an endpoint. The ultimate objective of this work is to better understand the neuroanatomic regions involved in post-RT memory decline and identify potential targets for memory-sparing brain RT.

# METHODS AND MATERIALS

## Standard Protocol Approvals and Patient Consents

This study was approved by our institutional review board. All participants provided written informed consent prior to participation.

## Study Design and Participants

Adults with primary brain tumors who were eligible for fractionated partial-brain RT with protons or photons (1.8-2.0 Gy per fraction, 50.4-60 Gy total dose) were enrolled in the parent prospective, observational study from 2014-2016. Eligibility criteria included age >18, Karnofsky performance status >70, ability to answer questions and follow commands in English at the time of consultation and treatment, and estimated life expectancy >1 year. Patients who received prior brain RT were excluded. Patients were studied at four time points: baseline (pre-RT), 3 months, 6 months, and 12 months post-RT. At each time point, high-resolution 3D volumetric brain MRI and diffusion-weighted imaging (DWI) were obtained (per clinical standard-of-care at our institution), and a battery of neurocognitive tests was administered.

## Memory Assessment

All participants underwent a 2-hour neuropsychological assessment at each time point. The battery included well-validated measures of verbal and visuospatial memory, executive functioning, and attention/processing speed, the domains that demonstrate greatest impairment in patients after brain RT[14]. The current analysis focused on a subset of the tests assessing verbal (Hopkins Verbal Learning Test-Revised [HVLT-R])[15] and visuospatial memory (Brief Visuospatial Memory Test-Revised [BVMT-R])[16]. These tests have alternate forms, which are ideal for repeat testing as different, but psychometrically equivalent, forms were used at each of the four time points to avoid patient “learning” of the tests. We analyzed structure-function associations that have been validated in previous studies (see eTable 1)[17–19].

Author Manuscript Author Manuscript Author Manuscript Author Manuscript

### Imaging Acquisition

High-resolution volumetric and diffusion-weighted MRI scans for all patients at each time point were acquired on a 3.0T 750 GE system (GE Healthcare, Milwaukee, Wisconsin) equipped with an 8-channel head coil. The imaging protocol included a 3D volumetric T1-weighted inversion recovery spoiled gradient echo sequence (echo time [TE]/repetition time [TR] = 2.8/6.5 ms; inversion time [TI] = 450 ms; flip angle = 8 degrees; field of view [FOV] = 24 cm) and a 3D FLAIR sequence (TE/TR = 125/6000 ms, TI = 1868 ms, FOV = 24 cm, matrix = 256×256, slice thickness = 1 mm). DWI was acquired with a single-shot pulsed-field gradient spin EPI sequence (TE/TR = 96 ms/17 s; FOV = 24 cm, matrix = 128 × 128 × 48; 1.87 × 1.875 in-plane resolution; slice thickness = 2.5 mm; 48 slices) with b = 0, 500, 1500, and 4000 s/mm2, with 1, 6, 6, and 15 unique gradient directions for each b-value respectively, and one average for each non-zero b-value. For use in nonlinear $B_0$ distortion correction, two additional b=0 volumes were acquired with either forward or reverse phase-encode polarity.

### Image Processing

The imaging data were preprocessed using in-house algorithms developed in MATLAB. Anatomical images were corrected for distortions due to gradient nonlinearities[20]. Diffusion scans were corrected for spatial distortions associated with gradient nonlinearities, susceptibility, and eddy currents[21,22]. *FreeSurfer, 5.3.0* was used to parcellate volumetric MRI into 34 cortical gyral-based ROIs[23]. Diffusion tensor imaging (DTI) maps of fractional anisotropy (FA) and mean diffusivity (MD) were derived by fitting the DWI data from b-values of 0, 500, and 1500 s/mm$^2$ to a tensor. In each voxel, the diffusion process is approximated by an ellipsoid defined by three perpendicular axes or eigenvectors. MD is a rotationally invariant measure of the average mobility of water molecules, calculated as an average of the three eigenvalues, and expressed as mm$^2$/sec. FA ranges from 0 to 1 as an expression of the degree of directional bias of diffusion.

Next, these DWI-derived maps were co-registered to high resolution volumetric MRI, and FA and MD values within the superficial white matter were calculated by sampling 5 mm below the WM surface normal at each vertex and then averaged within each ROI. Selected medial temporal lobe ROIs included the hippocampus and entorhinal, parahippocampal, and temporal pole WM (eTable 1; eFigure 1). These ROIs were preselected based on prior research implicating their role in the associated neurocognitive domains[17–19,24–26]. To avoid measuring tumor- or edema-related effects, a censoring mask including tumor, tumor bed, surgical cavity, surgical scars, and edema (T2 FLAIR hyperintensity) was manually drawn slice-by-slice on each image, and verified by two imaging experts. Voxels in the censoring mask were excluded from the final ROI to avoid confounding by tumor and edema-related effects[6].

### End Points

Change in each imaging parameter and memory measure were evaluated in two ways to capture the following: 1) subacute effects (i.e. change from baseline to 6 months post-RT), and 2) longitudinal evaluation of subacute and late-delayed effects, encompassing all time points (baseline, 3, 6, and 12 months post-RT). Reliable change indices (RCIs) were used to

Author Manuscript Author Manuscript Author Manuscript Author Manuscript

calculate neuropsychological change from baseline to 6 months post-RT, accounting for practice effects[27]. To evaluate time-dependent longitudinal performance, raw test scores and imaging parameters (FA and MD for WM, volume for gray matter) were analyzed. Raw neurocognitive test scores were used as opposed to age/education adjusted T scores so that we could independently investigate any associations between age, education, and outcome.

## Statistical Analysis

Statistics were performed in SPSS v24 (IBM Corp). To assess baseline to 6 months post-RT change, each parameter was evaluated by a one-sample t-test ($H_0$=0). Associations between subject characteristics (i.e. demographics, tumor type, chemotherapy) and 6-month changes in memory outcomes using RCIs were evaluated by Pearson correlations, independent sample t-tests, and one-way ANOVA.

To assess the main effects of time and imaging parameters as predictors of memory performance, random intercept and slope linear mixed effects (LME) models were performed:

$$\text{Memory Scores}_{ij} = (\beta_0 + b_{0i}) + (\beta_1 + b_{1i})\,\text{Month}_j + \beta_2\,\text{Imaging} + e_{ij}$$

where $b_{0i}$ = subject-specific random intercept, $b_{1i}$ = random slope, and $e_{ij}$ = subject error. This model was used to account for within-subject correlation between repeated measures, random subject intercepts, and incomplete outcomes (i.e. some patients were missing certain memory tests at certain time points, Supplemental eTable 2a). A random time component was specifically included to account for the change over time of the subjects.

In a separate analysis, the interaction between time and imaging parameters was included to evaluate whether the association between imaging and memory performance changes with time:

$$\text{Memory Scores}_{ij} = (\beta_0 + b_{0i}) + (\beta_1 + b_{1i})\,\text{Month}_j + \beta_2\,\text{Imaging} + \beta_3\,\text{Imaging} \times \text{Month}_j + e_{ij}$$

Outliers were identified and removed via Mahalanobis distance based on a chi-square distribution (assessed using $P$<.001)[28] Statistical significance was set at $\alpha$=0.05 for two-tailed tests.

Post-hoc analyses were done to further investigate time trends of neurocognitive performance in addition to evaluating baseline variability of particularly relevant clinical variables, namely age and tumor type. Based on significant baseline variability using independent sample t-tests, further analyses were performed including the significant baseline variables in the linear mixed effects models.

Author Manuscript Author Manuscript Author Manuscript Author Manuscript

## RESULTS

### Subacute Effects: Baseline to 6-Months Post-RT

Of the 56 subjects enrolled on the trial, 22 subjects had both pre- and 6 months post-RT imaging and memory assessments and were included in this analysis of subacute (baseline to 6-months post-RT) effects (eFigure 2). All subjects' raw scores at each time point are shown in eFigure 3.

Patient demographics and treatment characteristics are shown in Table 1. Notably, most patients were Non-Hispanic White. Most patients had a diagnosis of glioma and the minority had proton beam therapy as opposed to standard photon intensity modulated radiation therapy (IMRT). We noted that 14 patients (64%) were on anti-inflammatory corticosteroids and 10 (46%) had seizures at some point during the 6-month follow-up period.

Table 2 shows the mean dose delivered to each ROI. Mean doses to the left and right hippocampi were 13.8 Gy (SD=13.7) and 19.3 Gy (SD=18.0), respectively. Higher mean dose to the left temporal pole WM was significantly associated with decreased FA ($r$=−.667, $P$=.002).

When grouping by disease (glioma vs no glioma), there were some significant differences in baseline imaging parameters and memory performance. Specifically, patients with gliomas had significantly higher baseline right temporal pole MD values (mean difference $+5.25\times10^{-5}$, 95% CI [$1.76–8.73\times10^{-5}$], $P$=0.005). Patients with gliomas also had worse baseline performances of HVLT Total (mean difference −4.01, 95% CI [6.91, −1.10], $P$=0.009) and Delayed Recall (mean difference −2.31, 95% CI [−3.95,−0.66], $P$=0.008, equal variance not assumed).

Mean normalized changes in verbal and visuospatial memory from baseline to 6-months post-RT are summarized in Table 3. BVMT-R Total Recall declined from baseline (mean RCI= −1.34, 95% CI [−2.359, −0.328], $P$=.012). Older age was correlated with less 6-month decline in HVLT-R Total Recall ($r$=0.484, $P$=.026). This association remained significant ($P$=.021) on post-hoc analysis upon including baseline performance on HVLT-R Total Recall as a covariable. There was a strong trend for patients who had seizures to show a greater decline in BVMT-R Delayed Recall (mean RCI [$\bar{x}$]= −1.90, SD=2.92) than those without seizures ($\bar{x} = 0.30$, SD=1.98; t[19]=2.06, $P$=.053). Patients who received concurrent chemotherapy had a trend toward greater decline in visuospatial memory (BVMT-R Total Recall; $\bar{x} = -2.39$, SD=2.75) than patients not treated with concurrent chemotherapy ($\bar{x} = -0.40$, SD=1.02;, t[11.25]=2.15, $P$=.054). Levene's test indicated unequal variances (F=7.95, $P$=.011), so degrees of freedom were adjusted from 19 to 11.25.

### Neuroimaging Biomarkers of Memory Performance

**Linear Mixed Effects Analysis of Baseline to 12 Months Post-RT: Main Effects—**Of 56 patients enrolled, 27 subjects were eligible for the baseline to 12-month analyses (had at least two time points for both memory assessments and MRI over the 12-month study period). Supplemental eTable 2a provides information on missing data points in the

Author Manuscript



full longitudinal follow-up and eTable 2b details any significant differences in patient characteristics between subjects with and without missing data.

When considering all time points for each patient up to 12 months post-RT, the main effect of left hippocampal volume ($\beta_2$ in the linear mixed effects model) was not significantly associated with verbal memory performance (Figure 1). However, smaller right hippocampal volumes were associated with poorer BVMT-R Delayed Recall performance ($\beta_2$= 0.00214 points/mm$^3$, *P*=.021) and trended toward significantly associated with poorer BVMT-R Total Recall ($\beta_2$= 0.004 points/mm$^3$, *P*=.069)

Neither FA nor MD of left hemispheric WM within the parahippocampal, entorhinal, or temporal pole ROIs were associated with HVLT-R Total or Delayed Recall performance across time points (all *P*-values > .05). However, lower right entorhinal FA values and higher right entorhinal MD values were significantly associated with worse performance on BVMT-R Total Recall (β2= 49.15 points, *P*=.023; $\beta_2$= −28,385 points/mm$^2$/s, *P*=.047, respectively) (Figure 2). Higher right temporal pole MD values were significantly associated with poorer visuospatial memory (BVMT-R Total Recall, $\beta_2$= −60,800 points/mm$^2$/s, *P*=.003; BVMT-R Delayed Recall, $\beta_2$= −17,762 points/mm$^2$/s, *P*=.042). The main effect of time was not significantly associated with verbal or nonverbal memory.

On post-hoc analysis, time was evaluated without accounting for imaging parameters as shown in the following model:

$$\text{Memory Scores}_{ij} = (\beta_0 + b_{0i}) + (\beta_1 + b_{1i})\,\text{Month}_j + u_i + e_{ij}$$

HVLT Delayed Recall significantly declined over time ($\beta_1$ −0.14, *P*=0.018) (eFigure 3). When grouping the patients by age (old [60+] vs young), there were no significant differences in either baseline imaging parameters or neurocognitive tests (independent sample t-tests at P<0.05). Of note, despite baseline differences in imaging parameters and memory between patients with and without glioma, glioma was not a significant predictor of neurocognitive performance.

**Linear Mixed Effects Analysis of Baseline to 12 Months Post-RT: Time Interaction—**The interaction between left hippocampal volume and time was not significantly associated HVLT-R performances (Table 4). Similarly, the interactive effects of right hippocampal volume and time were not significantly associated with either BVMT-R Total Recall or Delayed Recall performance.

There were no significant interactions between left hemispheric WM and time. For right hemispheric WM, change in right temporal pole FA ($\beta_3$= −4.350 points/month, *P*=.024) and entorhinal MD ($\beta_3$= 2,868 points/[month*mm$^2$/s], *P*=.004) over the 12-month study period were associated with BVMT-R Delayed Recall performance. Entorhinal MD was also significantly associated with BVMT-R Total Recall ($\beta_3$= 5,523 points/[month*mm$^2$/s], *P*=.021).

Author Manuscript Author Manuscript Author Manuscript Author Manuscript

## DISCUSSION

In this prospective, longitudinal study of brain tumor patients undergoing RT, we demonstrate significant subacute decline in visuospatial, but not verbal, memory performance. To our knowledge, this is the first study to characterize the clinical and diffusion imaging predictors of longitudinal visuospatial memory, an important cognitive endpoint, in adult patients with primary brain tumors undergoing RT. Specifically, we found concurrent chemotherapy and the presence of seizures to be associated with greater decline in visuospatial memory at 6 months post-RT. Imaging biomarkers of damage to memory-associated gray and superficial WM structures in the right medial temporal lobe were significantly associated with poorer visuospatial memory performance. Time-dependent diffusion parameters indicating WM damage throughout the follow-up period also predicted visuospatial memory performance over 12 months.

Accounting for practice effects, verbal and visuospatial memory performance generally declined at 6 months post-RT, with a significant decline in visuospatial memory. This finding is consistent with previous studies noting impairment in verbal and visuospatial memory post-RT, in addition to decline in executive function, attention, and problem-solving[29]. Visuospatial memory, specifically, has not yet been prospectively investigated as a correlate of diffusion imaging changes in adult patients with primary brain tumors undergoing RT, although it has been evaluated among other patient populations (i.e., small cell lung cancer patients undergoing prophylactic cranial irradiation[30], pediatric patients with brain malignancies undergoing RT[31], and patients with mild cognitive impairment[32] and essential tremor[33]). We also found that older age was correlated with less decline in verbal memory, which differs from prior studies showing better performance of younger patients (<65 years) on both HVLT-R Total and Delayed Recall at 8 months after whole-brain radiation therapy[34]. The reason for this unexpected finding is unclear and cannot be explained by a higher functioning elderly cohort at baseline, thus it may reflect a greater cognitive reserve within our cohort of older patients. Seizures were associated with greater decline in visuospatial memory, aligning with previous literature on worse visuospatial performance in patients with several types of epilepsy[35]. Concurrent chemotherapy was associated with greater subacute effects on visuospatial memory, consistent with prior work showing that 30% of patients undergoing chemotherapy in addition to RT for brain tumors showed cognitive declines in visuospatial memory as well as verbal learning and memory, executive functioning, and processing speed[36]. This relationship is likely due to a shared mechanism for brain injury and cognitive decline between chemotherapy and radiation: interference of neural stem and precursor cell function[37].

Across all time points over 12 months post-RT, we demonstrated that damage to right medial temporal lobe gray and WM structures were associated with poorer visuospatial memory performance. Specifically, smaller right hippocampal volumes were associated with poorer visuospatial memory performance. The association between hippocampal volume loss and memory decline has been found in several patient populations, including Alzheimer disease[38], temporal pole epilepsy[39], and traumatic brain injury[40]. To our knowledge, this is the first study to show association between post-RT hippocampal atrophy and decline in memory performance in brain tumor patients on a clinical trial.

Author Manuscript Author Manuscript Author Manuscript Author Manuscript

Our finding of post-RT hippocampal atrophy is also supported by prior RT-specific work, such as hippocampal dose correlations with memory decline at 6 months post-RT[41] and 18 months post-fractionated stereotactic RT[42] and functional preservation in hippocampal-sparing WBRT at 4 months post-RT[43]. Despite the high frequency of hippocampal atrophy found in our cohort, the mean doses to the hippocampi in our cohort were much lower than previous studies[44], likely due to our study's strict inclusion criteria for hippocampal ROIs (censoring hippocampal regions with edema or proximity to the radiated surgical cavity). Nevertheless, our data suggest an association between radiation-associated hippocampal damage and the impairment of memory performance after brain RT.

Diffusion biomarkers of white matter injury in the right medial temporal lobe were also associated with visuospatial memory performance. Radiation damage to WM tracts is thought to be caused by demyelination, axonal injury, neuroinflammation, and vascular permeability, which can result in changes in diffusion properties such as decreased FA or increased MD[45]. Previous work has shown strong, dose-dependent diffusion changes post-RT in the fornix, cingulum bundle, and body of the corpus callosum[5]. We found that microstructural changes in the right entorhinal and temporal pole superficial WM are also associated with visuospatial memory performance. While previous studies have focused on tract-based analysis[5,6,10], we demonstrate the importance of WM directly beneath the cortex (i.e., superficial WM) as it enables communication across neighboring gyri in the form of U-fibers and may play a critical role in memory[46]. Although prior work and clinical trials have focused on hippocampal-sparing for cognitive preservation, damage to related afferent or efferent WM pathways may also contribute to radiation-induced memory impairment[47–49], thus understanding the relationship between the sensitivity of structures within the medial temporal lobe network to radiation may prove critical to strategies for improving brain tumor treatment.

Our investigation also demonstrated significant interactions between several right medial temporal lobe WM regions and time, indicating a change in the effect of diffusion imaging parameters on visuospatial memory over time post-RT. This relationship between higher right entorhinal MD and nonverbal memory performance at later time points may reflect the more chronic, progressive damage seen later (>6 months) in the post-RT chronology of radiation-induced tissue injury[1,50]. This "late delayed" brain injury is characterized by vascular abnormalities, demyelination, and even WM necrosis, which would be consistent with our findings of increased MD in the temporal pole WM[51,52]. Interestingly, the interaction between right-medial temporal pole FA and time showed the opposite directionality, which may be explained by dynamic changes in WM integrity longitudinally after RT, both chronologically and biologically. Indeed, subacute (~4–6 months post-RT) brain tissue damage (i.e. transient demyelination) can be reversible[1]. Thus, the counterintuitive direction of the association observed here may indicate more complex biologic processes occurring at later time points that defy our classic (and possibly simplistic) understanding of diffusion parameters. Previous work has reported an increase in FA post-RT in certain regions, which could be attributed to other, partially reversible biological processes involved in damage, such as undetected resolution of edema[53], axonal swelling as seen in traumatic brain injury[54], compression of peri-tumoral WM due to mass effect[55], or astrogliosis with compaction of axonal neurofilaments[56]. In addition, we may not

Author Manuscript Author Manuscript Author Manuscript Author Manuscript

expect to see consistent evidence of radiation-induced damage across all regions, since studies suggest that WM changes are not uniform for a given RT dose distribution[8,10,57].

This work has several limitations. The neuroanatomic atlas used to auto-segment ROIs with *FreeSurfer* was developed based on normal brain anatomy. However, this software is robust and well-validated, not subject to manual contouring differences, is used in other patient populations with neurological disorders[32,39,40], and has been used in several other published studies of brain tumor patients[58,59]. In addition, to minimize any potential segmentation error, all segmented images were carefully inspected slice-byslice, and we manually identified and censored areas of edema, tumor, and surgical cavities from all analyses, similar to previous studies[5,6,12]. As discussed, there was a greater censoring of hippocampi and WM regions receiving the highest dose due to potential structural changes from nearby tumor infiltration. Thus, we likely excluded tissue from analysis where we may have found stronger correlations between imaging biomarkers of damage and memory decline, yet the associations we did find are more robust and less likely to be due to tumor or edema-related processes. Also, given the complexity of verbal and visuospatial memory outcomes, other variables (e.g., co-morbid depression or anxiety) could have influenced memory performance and future analyses can incorporate such additional variables. Finally, while our sample size is limited, we present prospective results derived from robust neurocognitive testing and detailed, consistent neuroimaging of a relatively homogenous sample of brain tumor patients, which is rare in this realm of research. Some previous studies[41] combine several brain RT patient populations, including those who have received whole brain RT and partial brain RT, those with brain metastases and primary brain tumor patients. Though these limitations are worth noting, this prospective study with both detailed memory and imaging measures shows important associations between domain-specific neuroimaging biomarkers and cognitive performance after brain RT.

## CONCLUSIONS

Using advanced neuroimaging techniques, we found associations between imaging biomarkers and memory performance in patients with a primary brain tumor undergoing fractionated partial RT. Concurrent chemotherapy was associated with greater decline in visuospatial memory at 6 months post-RT. Reduced hippocampal volume, decreased entorhinal FA, and greater temporal pole MD predicted worse visuospatial memory performance. Longitudinal changes in WM diffusion predicted both verbal and visuospatial memory outcomes. These findings have clinical implications, indicating that memory preservation, particularly visuospatial memory, is reliant on a variety of both gray and WM regions.

The quantitative, domain-specific data acquired through these studies will improve our understanding of brain toxicity and cognitive decline associated with radiation dosage to non-targeted tissue and can provide the basis for evidence-based cognition-sparing brain radiotherapy. Interestingly, this study introduces an association between certain WM diffusion changes and radiation-induced memory decline, which may indicate that there are other ROIs not studied in this paper that should be investigated as potential vulnerable areas contributing to post-RT cognitive decline. Further research is needed to investigate the

Author Manuscript

Author Manuscript

Author Manuscript

Author Manuscript



dynamic trajectories of tissue response to radiation to better understand how MRI changes can be used to predict important neurocognitive trajectories post-treatment. Specifically, we must work to validate these associations by investigating how early imaging changes can act as biomarkers predicting subsequent memory decline on a per-patient basis. This research may support future work investigating dose-sparing protocols to avoid regions critical for memory during brain RT.

## Supplementary Material

Refer to Web version on PubMed Central for supplementary material.

## Acknowledgements

We thank Vinit Nalawade, Programmer Analyst, UC San Diego, for his assistance with programming and reviewing statistical analyses.

**Funding Sources:** The project described was partially supported by the National Institutes of Health, Grant TL1TR001443 (KRT), KL2TR00099 (JAH-G), UL1TR000100 (JAH-G), R01NS065838 (CRM) and TL1TR001443 (MT), and by American Cancer Society RSG-15-229-01-CCE (CRM). The content is solely the responsibility of the authors and does not necessarily represent the official views of the NIH or ACS.

## REFERENCES

1. Greene-Schloesser D, Robbins ME. Radiation-induced cognitive impairment-from bench to bedside. Neuro Oncol. 2012;14(SUPPL.4). doi:10.1093/neuonc/nos196.
2. Greene-Schloesser D, Robbins ME, Peiffer AM, Shaw EG, Wheeler KT, Chan MD. Radiation-induced brain injury: A review. Front Oncol. 2012;2:73-. [PubMed: 22833841]
3. Panagiotakos G, Alshamy G, Chan B, et al. Long-term impact of radiation on the stem cell and oligodendrocyte precursors in the brain. PLoS One. 2007;2(7). doi: 10.1371/journal.pone.0000588.
4. Wang S, Wu EX, Qiu D, Leung LHT, Lau HF, Khong PL. Longitudinal diffusion tensor magnetic resonance imaging study of radiation-induced white matter damage in a rat model. Cancer Res. 2009;69(3):1190–1198. doi:10.1158/0008-5472.CAN-08-2661. [PubMed: 19155304]
5. Connor M, Karunamuni R, McDonald C, et al. Dose-dependent white matter damage after brain radiotherapy. Radiother Oncol. 2016;121(2):209–216. doi:10.1016/j.radonc.2016.10.003. [PubMed: 27776747]
6. Connor M, Karunamuni R, McDonald C, et al. Regional susceptibility to dose-dependent white matter damage after brain radiotherapy. Radiother Oncol. 2017;123(2):209–217. doi:10.1016/j.radonc.2017.04.006. [PubMed: 28460824]
7. Nagesh V, Tsien CI, Chenevert TL, et al. Radiation-Induced Changes in Normal-Appearing White Matter in Patients With Cerebral Tumors: A Diffusion Tensor Imaging Study. Int J Radiat Oncol Biol Phys. 2008;70(4):1002–1010. doi:10.1016/j.ijrobp.2007.08.020. [PubMed: 18313524]
8. Chang Z, Kirkpatrick JP, Wang Z, Cai J, Adamson J, Yin F-F. Evaluating Radiation-induced White Matter Changes in Patients Treated with Stereotactic Radiosurgery Using Diffusion Tensor Imaging: A Pilot Study. Technol Cancer Res Treat. 2014;13(1):21–28. doi:10.7785/tcrt.2012.500358. [PubMed: 23862743]
9. Chapman CH, Nagesh V, Sundgren PC, et al. Diffusion tensor imaging of normal-appearing white matter as biomarker for radiation-induced late delayed cognitive decline. Int J Radiat Oncol Biol Phys. 2012;82(5):2033–2040. doi:10.1016/j.ijrobp.2011.01.068. [PubMed: 21570218]
10. Chapman C, Nazem-Zadeh M, Lee O, et al. Regional variation in brain white matter diffusion index changes following chemoradiotherapy: a prospective study using tract-based spatial statistics. PLoS One. 2013;8(3).

Author Manuscript Author Manuscript Author Manuscript Author Manuscript


11. Mabbott DJ, Noseworthy MD, Bouffet E, Rockel C. Diffusion tensor imaging after cranial radiation in children for medulloblastoma: Correlation with IQ. 2006:244–252. doi: 10.1215/15228517-2006-002.

12. Seibert TM, Karunamuni RA. Radiation dose-dependent hippocampal atrophy detected with longitudinal volumetric magnetic resonance imaging. Int J Radiat Oncol Biol Phys. 2016;97(2): 263–269. [PubMed: 28068234]

13. Gondi V, Pugh SL, Tome WA, et al. Preservation of memory with conformal avoidance of the hippocampal neural stem-cell compartment during whole-brain radiotherapy for brain metastases (RTOG 0933): A phase II multi-institutional trial. J Clin Oncol. 2014;32(34):3810–3816. doi: 10.1200/JCO.2014.57.2909. [PubMed: 25349290]

14. Meyers CA, Rock EP, Fine HA. Refining endpoints in brain tumor clinical trials. J Neurooncol. 2012;108(2):227–230. doi:10.1007/s11060-012-0813-8. [PubMed: 22451194]

15. Brandt J, Benedict R. Hopkins Verbal Learning Test--Revised: Professional Manual. Psychological Assessment Resources; 2001.

16. Benedict R Brief Visuospatial Memory Test--Revised: Professional Manual. PAR; 1997.

17. Kucukboyaci NE, Girard HM, Hagler DJ, et al. Role of frontotemporal fiber tract integrity in task-switching performance of healthy controls and patients with temporal lobe epilepsy. J Int Neuropsychol Soc. 2012;18(1):57–67. doi:10.1017/S1355617711001391. [PubMed: 22014246]

18. McDonald CR, Ahmadi ME, Hagler DJ, et al. Diffusion tensor imaging correlates of memory and language impairments in temporal lobe epilepsy. Neurology. 2008;71 (23):1869–1876. doi: 10.1212/01.wnl.0000327824.05348.3b. [PubMed: 18946001]

19. Peiffer AM, Leyrer CM, Greene-Schloesser DM, et al. Neuroanatomical target theory as a predictive model for radiation-induced cognitive decline. Neurology. 2013;80(8):747–753. doi: 10.1212/WNL.0b013e318283bb0a. [PubMed: 23390169]

20. Jovicich J, Czanner S, Greve D, et al. Reliability in multi-site structural MRI studies: Effects of gradient non-linearity correction on phantom and human data. Neuroimage. 2006;30(2):436–443. doi:10.1016/j.neuroimage.2005.09.046. [PubMed: 16300968]

21. Holland D, Kuperman JM, Dale AM. Efficient correction of inhomogeneous static magnetic field-induced distortion in Echo Planar Imaging. Neuroimage. 2010;50(1):175–183. doi:10.1016/j.neuroimage.2009.11.044. [PubMed: 19944768]

22. Zhuang J, Hrabe J, Kangarlu A, et al. Correction of eddy-current distortions in diffusion tensor images using the known directions and strengths of diffusion gradients. J Magn Reson Imaging. 2006;24(5):1188–1193. doi:10.1002/jmri.20727. [PubMed: 17024663]

23. Desikan RS, Ségonne F, Fischl B, et al. An automated labeling system for subdividing the human cerebral cortex on MRI scans into gyral based regions of interest. Neuroimage. 2006;31(3):968–980. doi:10.1016/j.neuroimage.2006.01.021. [PubMed: 16530430]

24. Meyers CA, Brown PD. Role and relevance of neurocognitive assessment in clinical trials of patients with CNS tumors. J Clin Oncol. 2006;24(8):1305–1309. doi:10.1200/JCO.2005.04.6086. [PubMed: 16525186]

25. Fischl B, Van Der Kouwe A, Destrieux C, et al. Automatically Parcellating the Human Cerebral Cortex. Cereb Cortex. 2004;14(1):11–22. doi: 10.1093/cercor/bhg087. [PubMed: 14654453]

26. Rodríguez-Cruces R, Concha L. White matter in temporal lobe epilepsy: clinico-pathological correlates of water diffusion abnormalities. Quant Imaging Med Surg. 2015;5(2):264–278. doi: 10.3978/j.issn.2223-4292.2015.02.06. [PubMed: 25853084]

27. Chelune GJ, Naugle RI, Lüders H, Sedlak J, et al. Individual change after epilepsy surgery: Practice effects and base-rate information. Neuropsychology. 1993;7:41–52. doi: 10.1037/0894-4105.7.1.41.

28. Mahalanobis P On tests and measures of groups divergence. J Asiat Sociol Bengal. 1930;26:541–588.

29. Crossen J, Garwood D, Glatstein E, Neuwelt E. Neurobehavioral sequelae of cranial irradiation in adults: a review of radiation-induced encephalopathy. J Clin Oncol. 1994;12:627–642. [PubMed: 8120563]

30. Simó M, Vaquero L, Ripollés P, et al. Longitudinal Brain Changes Associated with Prophylactic Cranial Irradiation in Lung Cancer. J Thorac Oncol. 2016;11(4):475–486. [PubMed: 26804637]

Author Manuscript Author Manuscript Author Manuscript Author Manuscript

31. Horska A, Nidecker A, Intrapiromkul J, et al. Diffusion Tensor Imaging of Deep Gray Matter in Children Treated for Brain Malignancies. Childs Nerv Syst. 2014;30(4):631–638. [PubMed: 24264381]

32. Mitolo M, Gardini S, Fasano F, et al. Visuospatial Memory and Neuroimaging Correlates in Mild Cognitive Impairment. J Alzheimer's Dis. 2013;35(1):75–90. [PubMed: 23357899]

33. Benito-Leon J, Mato-Abad V, Louis E, et al. White matter microstructural changes are related to cognitive dysfunction in essential tremor. Sci Rep. 2017;7. [PubMed: 28127057]

34. Saito H, Tanaka K, Kanemoto A, Nakano T, Abe E, Aoyama H. Factors Affecting the Baseline and Post-Treatment Scores on the Hopkins Verbal Learning Test-Revised Japanese Version before and after Whole-Brain Radiation Therapy. Int J Mol Sci. 2016;17(11).

35. Chin J, Scharfman H. Shared cognitive and behavioral impairments in epilepsy and Alzheimer's disease and potential underlying mechanisms. Epilepsy Behav. 2013;26(3):343–351. [PubMed: 23321057]

36. Schagen S, Wefel J. Chemotherapy-related changes in cognitive functioning. EJC Suppl. 2013;11(2):225–232. [PubMed: 26217131]

37. Gibson E, Monje M. Effect of cancer therapy on neural stem cells: implications for cognitive function. Curr Opin Oncol. 2012;24(6):672–678. doi: 10.1097/CCO.0b013e3283571a8e. [PubMed: 22913969]

38. Heister D, Brewer JB, Magda S, Blennow K, McEvoy LK. Predicting MCI outcome with clinically available MRI and CSF biomarkers. Neurology. 2011 ;77(17): 1619–1628. doi:10.1212/WNL.0b013e3182343314. [PubMed: 21998317]

39. Farid N, Girard HM, Kemmotsu N, et al. Temporal Lobe Epilepsy: Quantitative MR Volumetry in Detection of Hippocampal Atrophy. Radiology. 2012;264(2):542–550. doi: 10.1148/radiol.12112638. [PubMed: 22723496]

40. Brezova V, G??ran Moen K, Skandsen T, et al. Prospective longitudinal MRI study of brain volumes and diffusion changes during the first year after moderate to severe traumatic brain injury. NeuroImage Clin. 2014;5:128–140. doi:10.1016/j.nicl.2014.03.012. [PubMed: 25068105]

41. Ma T, Grimm J, McIntyre R, et al. A prospective evaluation of hippocampal radiation dose volume effects and memory deficits following cranial irradiation. Radiother Oncol. 2017;125(2):234–240. [PubMed: 29128167]

42. Gondi V, Hermann BP, Mehta MP, Tomé WA. Hippocampal dosimetry predicts neurocognitive function impairment after fractionated stereotactic radiotherapy for benign or low-grade adult brain tumors. Int J Radiat Oncol Biol Phys. 2013;85(2):345–354. doi:10.1016/j.ijrobp.2012.11.031.

43. Tsai P-FT, Yang CC, Chuang C-C, Lin S-Y. Hippocampal dosimetry correlates with the change in neurocognitive function after hippocampal sparing during whole brain radiotherapy: A prospective study. Radiat Oncol. 2015; 10(1).

44. Chapman C, Nagesh V, Sundgren P, et al. Diffusion tensor imaging of normal-appearing white matter as biomarker for radiation-induced late delayed cognitive decline. Int J Radiat Oncol Biol Phys. 2012;82:2033–2040. [PubMed: 21570218]

45. Connor M, Karunamuni R, McDonald C, et al. Dose-dependent white matter damage after brain radiotherapy. Radiother Oncol. 2016;121(2):209–216. doi:10.1016/j.radonc.2016.10.003. [PubMed: 27776747]

46. Nazeri A, Chakravarty MM, Rajji TK, et al. Superficial white matter as a novel substrate of age-related cognitive decline. Neurobiol Aging. 2015;36(6):2094–2106. doi:10.1016/j.neurobiolaging.2015.02.022. [PubMed: 25834938]

47. Nagesh V, Tsien CI, Chenevert TL, et al. Radiation-Induced Changes in Normal-Appearing White Matter in Patients With Cerebral Tumors: A Diffusion Tensor Imaging Study. Int J Radiat Oncol Biol Phys. 2008;70(4):1002–1010. doi:10.1016/j.ijrobp.2007.08.020. [PubMed: 18313524]

48. Welzel T, Niethammer A, Mende U, Heiland S, Wenz F, Debus J. Diffusion tensor imaging screening of radiation-induced changes in the white matter after prophylactic cranial irradiation of patients with small cell lung cancer: first results of a prospective study. AJNR Am J Neuroradiol. 2008;29:379–383. [PubMed: 17974610]

Author Manuscript Author Manuscript Author Manuscript Author Manuscript

49. Nazem-Zadeh M-R, Chapman CH, Lawrence TL, Tsien CI, Cao Y. Radiation therapy effects on white matter fiber tracts of the limbic circuit. Med Phys. 2012;39(9):5603. doi:10.1118/1.4745560. [PubMed: 22957626]

50. Tofilon PJ, Fike JR. The radioresponse of the central nervous system: a dynamic process. Radiat Res. 2000;153(4):357–370. doi:10.1667/0033-7587(2000)153[0357:TROTCN]2.0.CO;2. [PubMed: 10798963]

51. Schultheiss TE, Stephens LC. Invited review: Permanent radiation myelopathy. Br J Radiol. 1992;65(777):737–753. doi:10.1259/0007-1285-65-777-737. [PubMed: 1393407]

52. Lee YW, Cho HJ, Lee WH, Sonntag WE. Whole brain radiation-induced cognitive impairment: pathophysiological mechanisms and therapeutic targets. Biomol Ther (Seoul). 2012;20(4):357–370. doi:10.4062/biomolther.2012.20.4.357. [PubMed: 24009822]

53. Armitage PA, Bastin ME, Marshal I, Wardlaw JM, Cannon J. Diffusion anisotropy measurements in ischaemic stroke of the human brain. Magn Reson Mater Physics, Biol Med. 1998;6(1):28–36. doi:10.1016/S1352-8661(98)00007-6.

54. Roberts RM, Mathias JL, Rose SE. Diffusion Tensor Imaging (DTI) Findings Following Pediatric Non-Penetrating TBI: A Meta-Analysis. Dev Neuropsychol. 2014;39(8):600–637. doi: 10.1080/87565641.2014.973958. [PubMed: 25470224]

55. Chenevert TL, Ross BD. Diffusion Imaging for Therapy Response Assessment of Brain Tumor. Neuroimaging Clin N Am. 2009;19(4):559–571. doi: 10.1016/j.nic.2009.08.009. [PubMed: 19959005]

56. Croall ID, Cowie CJA, He J, et al. White matter correlates of cognitive dysfunction after mild traumatic brain injury. Neurology. 2014;83(6):494–501. doi:10.1212/WNL.0000000000000666. [PubMed: 25031282]

57. Uh J, Merchant TE, Li Y, et al. Differences in brainstem fiber tract response to radiation: A longitudinal diffusion tensor imaging study. Int J Radiat Oncol Biol Phys. 2013;86(2):292–297. doi:10.1016/j.ijrobp.2013.01.028. [PubMed: 23474114]

58. Karunamuni R, Bartsch H, White NS, et al. Dose-Dependent Cortical Thinning After Partial Brain Irradiation in High-Grade Glioma. Radiat Oncol Biol. 2016;94(2):297–304. doi:10.1016/j.ijrobp.2015.10.026.

59. Seibert T, Karunamuni R, Kaifi S, Burkeen J, Krishnan A, Hattangadi J. Selective Vulnerability of Cerebral Cortex Regions to Radiation Dose-Dependent Atrophy. Int J Radiat Oncol Biol Phys. 2016;96(2).

Author Manuscript
Author Manuscript
Author Manuscript
Author Manuscript

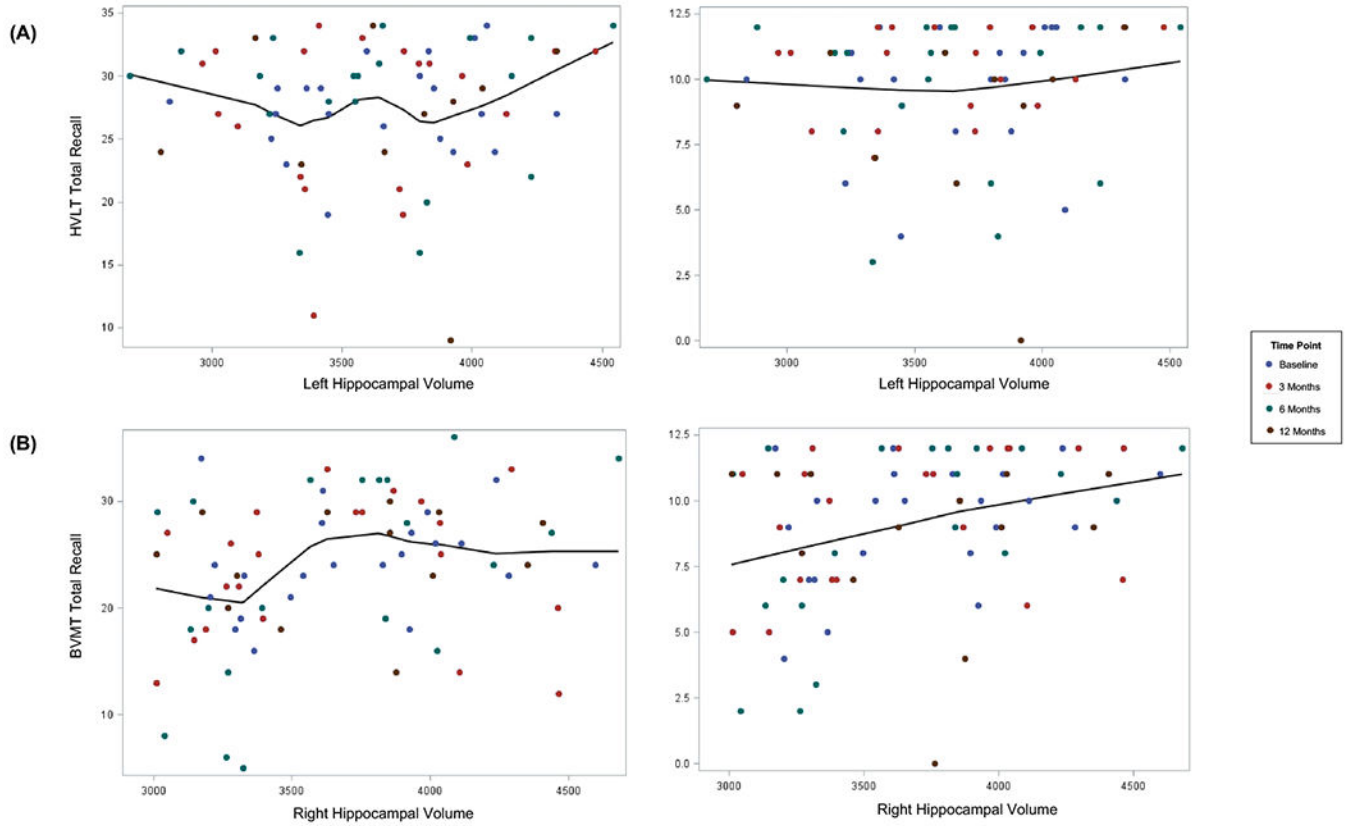


**Figure 1.**
Scatter plots for hippocampal volume and domain-specific memory performance including all time points for each patient up to 12 months post-RT. The trend line overlays the LOESS fit with the smoothing parameter that minimizes the AICC criterion. Significant associations between imaging parameter and memory test were determined based on the beta coefficient ($\beta_2$) derived from the linear mixed effects model with random intercept and slope:

$$\text{Memory Scores}_{ij} = (\beta_0 + b_{0i}) + (\beta_1 + b_{1i})\,\text{Month}_j + \beta_2\,\text{Imaging} + e_{ij}$$

Raw memory scores are shown. Hippocampal volumes are shown as $mm^3$.
**(A)** Smaller left hippocampal volumes were not significantly associated with poorer performance on verbal memory testing (HVLT-R Total Recall $\beta_2$= 0.00038, *P*=.849; HVLT-R Delayed Recall, $\beta_2$= 0.00008, *P*=.935).
**(B)** Smaller right hippocampal volumes were significantly associated with worse performance on visuospatial memory testing (BVMT-R Total Recall, $\beta_2$= 0.004 points/$mm^3$, *P*=.069; BVMT-R Delayed Recall, $\beta_2$= 0.00214 points/$mm^3$, *P*=.021). Abbreviations: BVMT-R, Brief Visuospatial Memory Test-Revised; HVLT-R, Hopkins Verbal Learning Test-Revised

Author Manuscript Author Manuscript Author Manuscript Author Manuscript

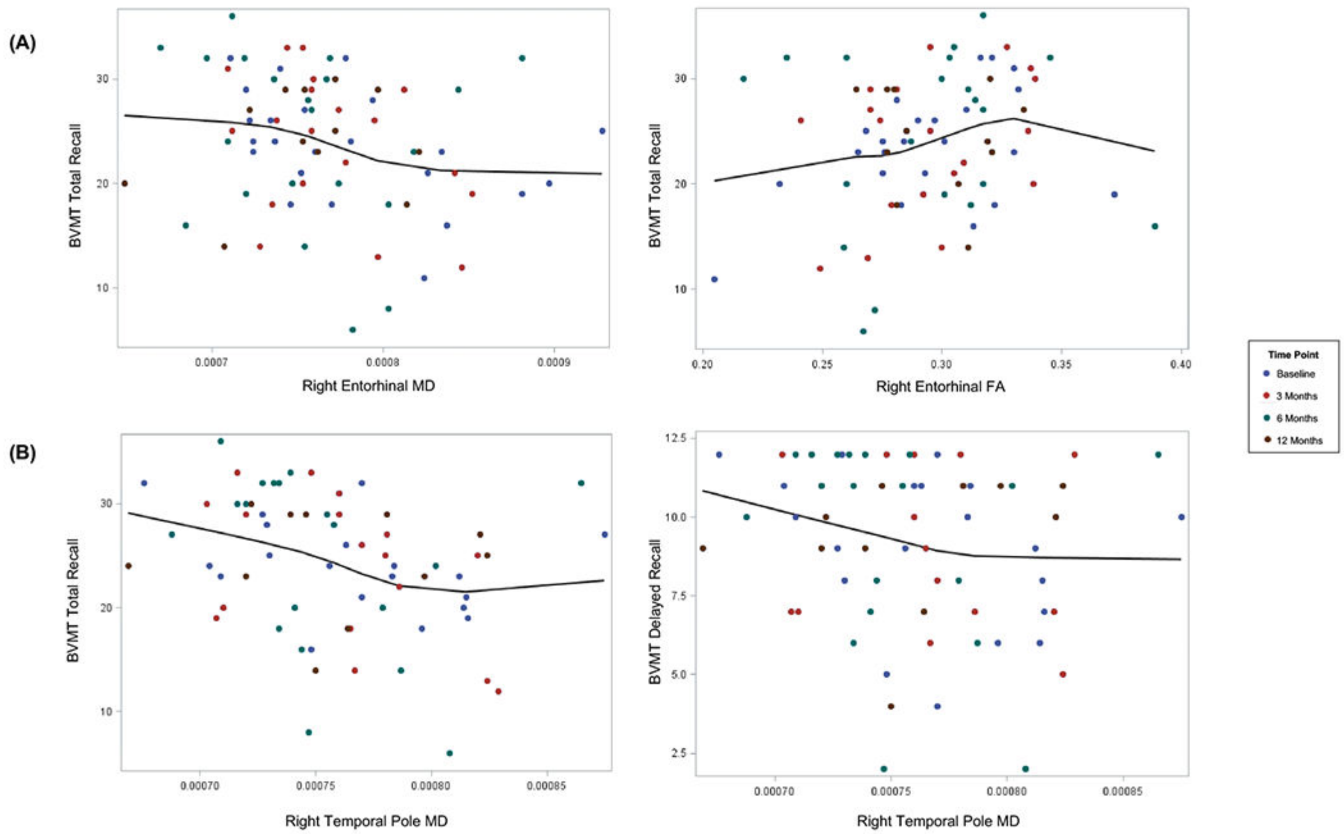


**Figure 2.**

Scatter plots for **(A)** right entorhinal and **(B)** right temporal WM and visuospatial memory performance including all time points for each patient up to 12 months post-RT. The trend line overlays the LOESS fit with the smoothing parameter that minimizes the AICC criterion. Significant associations between imaging parameter and memory test were determined based on the beta coefficient ($\beta_2$) derived from the linear mixed effects model with random intercept and slope:

$$\text{Memory Scores}_{ij} = (\beta_0 + b_{0i}) + (\beta_1 + b_{1i})\ \text{Month}_j + \beta_2\ \text{Imaging} + e_{ij}$$

Raw memory scores are shown. MD is expressed in $mm^2/s$. FA is unitless. Outliers (n=2 and n=4 for **A** and **B**, respectively) were removed based on statistically significantly great Mahalanobis distances ($P$<.001).

**(A)** Higher right entorhinal MD values were significantly associated with worse BVMT-R Total Recall ($\beta_2$= −28,385 points/$mm^2$/s, $P$=.047). Smaller right entorhinal FA values were significantly associated with worse BVMT-R Total Recall ($\beta_2$= 49.15 points,$P$=.023). **(B)** Higher right temporal pole MD values were significantly associated with worse nonverbal memory (BVMT-R Total Recall, $\beta_2$= −60,800 301 points/$mm^2$/s , $P$=.003; BVMT-R Delayed Recall, $\beta_2$= −17,762 301 points/$mm^2$/s, $P$=.042).

Abbreviations: BVMT-R, Brief Visuospatial Memory Test-Revised; HVLT-R, Hopkins Verbal Learning Test-Revised

Author Manuscript
Author Manuscript
Author Manuscript
Author Manuscript

**Table 1.**

Subject and cancer characteristics (N=22)

| **Demographic** | **Patients, No. (%)** |
|---|---|
| Gender | |
| Men | 11 (50.0) |
| Women | 11 (50.0) |
| Race | |
| Non-Hispanic White | 18 (81.8) |
| Black | 1 (4.5) |
| Hispanic | 3 (13.6) |
| Age (median, range) | 48 (20, 75) |
| Education, years (median, range) | 14 (10, 20) |
| **Cancer or Treatment Characteristic** | **Patients, No. (%)** |
| Glioma | 14 (63.6) |
| Laterality | |
| Left | 7 (31.8) |
| Right | 10 (45.5) |
| Bilateral | 5 (22.7) |
| Radiation Therapy | |
| Proton Beam Therapy | 7 (31.8) |
| IMRT | 15 (68.2) |
| Radiotherapy Prescription Dose (median [Gy], range) | 54.0 (50.4, 60.0) |
| Chemotherapy | |
| Concurrent | 11 (50.0) |
| Adjuvant | 13 (59.0) |
| Steroids | 12 (54.5) |
| Seizures | 10 (45.5) |

Abbreviations: N, number; IMRT, intensity modulated radiation therapy; Gy, Grey

Author Manuscript Author Manuscript Author Manuscript Author Manuscript

**Table 2.**

Mean dose and imaging parameter by region

| Structure | Sample Size* (N) | Mean Dose (mean Gy, SD) | Percent Change in Volume (mean %, SD) / Number Atrophied (%) | Percent Change in MD (mean %, SD) | Percent Change in FA (mean %, SD) |
|---|---|---|---|---|---|
| **Left hippocampus** | 18 | 13.8 (13.7) | −2 (17) / 9 (50) | - | - |
| **Right hippocampus** | 19 | 19.3 (18.0) | +4 (28) / 10 (53) | - | - |
| **Left WM** | | | | | |
| **Entorhinal** | 19 | 20.4 (20.9) | - | 17 (8) | −16 (23) |
| **Parahippocampal** | 19 | 22.6 (23.2) | - | −5 (8) | 6 (27) |
| **Temporal pole** | 18 | 24.8 (20.0) | - | 15 (8) | −10 (5) |
| **Right WM** | | | | | |
| **Entorhinal** | 18 | 23.8 (18.9) | - | 19 (10) | −16 (15) |
| **Parahippocampal** | 19 | 24.5 (22.2) | - | −8 (10) | 11 (11) |
| **Temporal pole** | 19 | 24.8 (20.0) | - | 16 (7) | −31 (15) |

*The analytic sample size is less than the total eligible sample size of 22 subjects due to censoring.

Percent change is shown from baseline to 6 months (i.e. a negative value represents a decrease over time). Abbreviations: SD, standard deviation; WM, white matter; Gy, Grey; FA, fractional anisotropy; MD, mean diffusivity.

Author Manuscript


### Table 3.

Change in neurocognitive tests at 6 months post-RT from baseline

| Memory Test | Mean RCI (95% CI) | *P*-value* |
|---|---|---|
| **Verbal Memory** | | |
| HVLT-R Total Recall | −0.013 [−0.709, 0.682] | 0.968 |
| HVLT-R Delayed Recall | −0.104 [−0.602, 0.394] | 0.667 |
| **Visuospatial Memory** | | |
| BVMT-R Total Recall | −1.343 [−2.359, −0.328] | 0.012 † |
| BVMT-R Delayed Recall | −0.645 [−1.835, 0.544] | 0.271 |

Abbreviations: RT, radiotherapy; BVMT-R, Brief Visuospatial Memory Test-Revised; HVLT-R, Hopkins Verbal Learning Test-Revised; RCI, Reliable Change Index

* *P*-value represents one sample T test ($H_0$=0, no change from baseline).

† Significant at *P*<.05.

Author Manuscript Author Manuscript Author Manuscript Author Manuscript

**Table 4.**

Interactions between imaging biomarkers and time

| Right-hemispheric Structure | Imaging Biomarker | BVMT-R Total Recall: β Interaction* | *P*-value | BVMT-R Delayed Recall: β Interaction | *P*-value |
|---|---|---|---|---|---|
| Hippocampus | Volume | 0.0002 | 0.548 | −.0001 | 0.405 |
| Entorhinal WM | FA | −7.547 | 0.102 | −2.450 | 0.188 |
| | MD | **5,523** | **0.021**† | **2,868** | **0.004**† |
| Parahippocampal WM | FA | −1.788 | 0.705 | −3.378 | 0.067 |
| | MD | 3,504 | 0.262 | 1,450 | 0.213 |
| Temporal Pole WM | FA | −4.166 | 0.380 | **−4.350** | **0.024**† |
| | MD | 1,955 | 0.424 | 1,905 | 0.087 |
| **Left-hemispheric Structure** | **Imaging Biomarker** | **HVLT-R Total Recall: β Interaction** | ***P*-value** | **HVLT-R Delayed Recall:** | ***P*-value** |
| Hippocampus | Volume | −0.0001 | 0.730 | −0.00001 | 0.467 |
| Entorhinal WM | FA | 2.411 | 0.599 | −1.095 | 0.641 |
| | MD | 408.2 | 0.923 | 808.0 | 0.690 |
| Parahippocampal WM | FA | 1.423 | 0.773 | 1.225 | 0.629 |
| | MD | −7,336 | 0.089 | −2,916 | 0.197 |
| Temporal Pole WM | FA | 0.4000 | 0.939 | −0.075 | 0.976 |
| | MD | −4,782 | 0.174 | −3,029 | 0.098 |

*Where the interaction coefficient is $\beta_3$ in the following linear mixed effects model:

$$\text{Memory Scores}_{ij} = (\beta_0 + b_{0i}) + (\beta_1 + b_{1i})\,\text{Month}_j + \beta_2\ \text{Imaging} + \beta_3 \text{Imaging} \times \text{Month}_j + e_{ij}$$

where $b_{0i}$ = subject-specific random intercept, $b_{1i}$ = random slope, and $e_{ij}$ = subject error. The $\beta_3$ interaction coefficient has the units: volume, points/(month*mm$^3$); FA, points/month; MD, points/(month*mm$^2$/s)

†*P*-value significant at alpha = 0.05